Coherent 420 nm laser beam generated by four-wave mixing in Rb vapor with a single continuous-wave laser*

Hao Liu(刘浩)[1,2], Jin-Peng Yuan(元晋鹏)[1,2,†], Li-Rong Wang(汪丽蓉)[1,2,‡], Lian-Tuan Xiao(肖连团)[1,2], and Suo-Tang Jia(贾锁堂)[1,2]

[1] *State Key Laboratory of Quantum Optics and Quantum Optics Devices, Institute of Laser Spectroscopy, Shanxi University, Taiyuan* 030006, *China*
[2] *Collaborative Innovation Center of Extreme Optics, Shanxi University, Taiyuan* 030006, *China*

(Received 7 January 2020; revised manuscript received 4 February 2020; accepted manuscript online 13 February 2020)

We demonstrate the generation of the coherent 420 nm laser via parametric four-wave mixing process in Rb vapor. A single 778 nm laser with circular polarization is directly injected into a high-density atomic vapor, which drives the atoms from the $5S_{1/2}$ state to the $5D_{5/2}$ state with monochromatic two-photon transition. The frequency up-conversion laser is generated by the parametric four-wave mixing process under the phase matching condition. This coherent laser is firstly certified by the knife-edge method and a narrow range grating spectrometer. Then the generated laser power is investigated in terms of the power and frequency of the incoming beam as well as the density of the atoms. Finally, a 420 nm coherent laser with power of 19 μW and beam quality of $M_x^2 = 1.32$, $M_y^2 = 1.37$ is obtained with optimal experimental parameters. This novel laser shows potential prospects in the measurement of material properties, information storage, and underwater optical communication.

Keywords: blue laser, four-wave mixing, frequency up-conversion

PACS: 32.80.–t, 42.65.–k, 42.65.Ky **DOI:** 10.1088/1674-1056/ab75d9

1. Introduction

Nonlinear optical processes in an atomic medium give rise to fascinating phenomena such as coherent population trapping,[1] electromagnetically induced transparency,[2] lasing without inversion,[3] and multi-wave mixing.[4] Among different nonlinear optical processes in the atomic medium, frequency conversion is widely studied as a promising approach for studying the physical process itself and attaining novel wavelength lasers.

In addition to traditional nonlinear crystals, a strong nonlinearity can be achieved in the proximity of optical transitions in the atomic medium as well, which has shown potentials in a wide range of applications, such as quantum information science,[5] coherent optical phenomena diagnostic,[6] and generation of novel tunable laser sources. Especially, most optical detectors are very sensitive to the blue light field (400–480 nm) which can be obtained by the infrared field up-conversion. Therefore, the frequency conversion effect has great future in night vision,[7] star studies,[8] underwater communication,[9] etc. There have been extensive studies of the transitions in atomic medium[10,11] that appear suitable for the frequency up-conversion, and the efficiency can be improved dramatically by controlling the parametric four-wave mixing (FWM) process.

Since the FWM process in atomic medium has been proved as a useful method for producing short wavelength laser beams, it has been paid more attention in recent studies. Using multiple near-infrared fields to generate blue and mid-infrared radiations by FWM in Rb vapor was pioneered by Zibrov *et al.*[12] and then achieved in cesium medium.[13] Also, another additional resonant laser was demonstrated as a useful way to enhance the power of the blue laser.[14] However, the requirement of multiple pump lasers increases the complexity of the system, which sets an obstacle for the applications based on the blue laser. Sulham *et al.* investigated the generation of a blue laser by using a single dye laser in rubidium and cesium medium.[15] While, the linewidth of the dye laser is usually several GHz, which has a direct defective influence on the linewidth of the generated blue laser. Compared with pulsed laser, single continue wavelength laser has advantages of distinct narrow linewidth and convenient equipment integration. A preliminary research was carried out in ^{87}Rb isotopes recently.[16] However, a further and detailed research about the efficient generation of this specific blue light with a single laser beam is still required for underwater communication or other potential applications.

In this work, we investigate the efficient frequency up-conversion in a thermal vapor containing a natural mixture of

*Project supported by the National R&D Program of China (Grant No. 2017YFA0304203), the National Natural Science Foundation of China (Grant Nos. 61875112, 61705122, 91736209, and 61728502), the Program for Sanjin Scholars of Shanxi Province, China, the Applied Basic Research Project of Shanxi Province, China (Grant No. 201701D221004), the Key Research and Development Program of Shanxi Province for International Cooperation, China (Grant No. 201803D421034), and 1331KSC.

†Corresponding author. E-mail: yjp@sxu.edu.cn
‡Corresponding author. E-mail: wlr@sxu.edu.cn

^{85}Rb and ^{87}Rb isotopes via a parametric FWM process. The spatial and spectral measurements of the generated beam were implemented by using a knife-edge method and a narrow range grating spectrometer, which confirm that the novel light is a collimated and single-wavelength coherent 420 nm laser. The relationship between the generated blue laser and various experimental parameters was studied in detail. In this parametric FWM process, the appropriate parameters can facilitate the generation of the blue laser, which shows promises in communication between near-infrared and blue light fields.

2. Experimental setup

The related energy levels of the FWM process are shown in Fig. 1(a). The two-photon transition is achieved via the simultaneous absorptions of two 778 nm photons, which excite the rubidium atoms from the $5S_{1/2}$ ground state to the $5D_{5/2}$ excited state. A third optical field of 5.2 μm infrared radiation is firstly generated corresponding to the $5D_{5/2} \rightarrow 6P_{3/2}$ transition. Then the strong atomic coherence in this diamond-type energy level structure produces the collimated blue light (CBL) at 420 nm via the parametric FWM process corresponding to the $6P_{3/2} \rightarrow 5S_{1/2}$ transition.

A schematic experimental setup is shown in Fig. 1(b). The pump laser is provided by a diode laser (DLC TA pro, Toptica), with a tunable range of 30 nm and a linewidth less than 1 MHz. After the laser passes through a single-mode polarization-maintaining fiber, a 778 nm Gaussian beam with the power of 1.3 W and beam quality of $M_x^2 = 1.24$, $M_y^2 = 1.35$ is obtained. A half wave plate (HWP1) and a polarization beam splitter (PBS1) are used to divide a weak beam from the main beam. The laser frequency is precisely monitored by a wavelength meter (WS-7, High Finesse). Then the main beam is split into two beams by HWP2 and the PBS2 with different powers. One beam with the power of about 30 mW is used to obtain the reference two-photon transition spectroscopy in vapor A which is 50 mm in length and 25 mm in diameter. The vapor is shielded with a μ-metal to reduce the effect of stray magnetic field and the temperature can be accurately controlled by a self-feedback temperature controller (TC1). The 420 nm fluorescence from the cascade decay of the upper $5D_{5/2}$ state is fltered with an interference filter (center wavelength 420 nm, 10 nm pass band) to isolate the background light, and then detected by a side-window photomultiplier tube (CR131, Hamamatsu). The other strong 778 nm beam with circular polarization is used to generate the CBL with the phase match of the FWM process. Meanwhile, a high atomic density for realizing the parametric FWM process is achieved by a self-feedback temperature controller (TC2).

At the exit of vapor B, we block the transmitted input pump laser by using two dichroic mirrors and a 420 nm bandpass interference filter. The generated laser beam is firstly measured by a narrow range grating spectrometer (AvaSpec-ULS2048L, Avantes). Then, the knife-edge method, which is implemented by a chopper wheel (SR540, Stanford Research Systems) and a photodiode (PDA36A-EC, Thorlabs), is also used to demonstrate the blue laser. Finally, we evaluate the beam quality M^2 of the generated coherent radiation by using a CCD. The power of the generated laser is measured by using a power meter (S305C, Thorlabs).

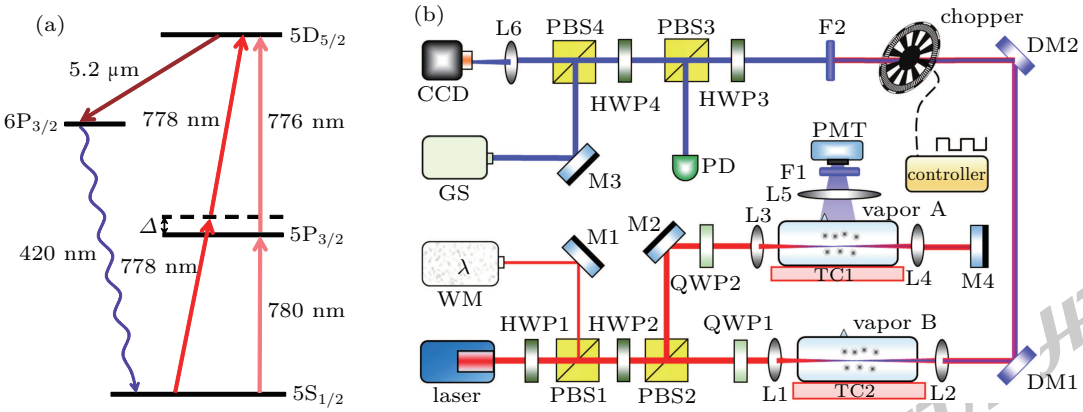

Fig. 1. (a) The energy levels involved in the parametric FWM process of rubidium atoms. (b) Experimental setup. L: lens, F: 420 nm bandpass interference filter; M: high reflection mirror, PMT: photomultiplier tube, DM: dichroic mirror, HWP: half-wave plate, QWP: quarter-wave plate, PBS: polarization beam splitter, PD: photodiode, TC: temperature controller, WM: wavelength meter, GS: narrow range grating spectrometer, CCD: charge coupled device.

3. Results and analysis

The coherent 420 nm laser is generated via parametric FWM process by a single 778 nm laser in Rb vapor. The beam is observed at the exit of vapor B in the same propagating direction as the input pump beam. The beam's spatial profile can be characterized by using the knife-edge method.[17,18] A chopper with modulation frequency of 30 Hz is used in the experiment. Figure 2(a) presents the normalized intensities of the 778 nm pump beam (black line) and 420 nm blue beam (red line), respectively. The measurement results show that the

two beams spatially overlap with each other. The directionality of the generated blue beam is consistent with the phase matching condition for FWM, $\boldsymbol{k}_{\rm pump} + \boldsymbol{k}_{\rm pump} = \boldsymbol{k}_{\rm ir} + \boldsymbol{k}_{\rm cbl}$, where $\boldsymbol{k}_{\rm pump}$, $\boldsymbol{k}_{\rm ir}$, and $\boldsymbol{k}_{\rm cbl}$ are the wave vectors of the radiation at 778 nm, 5.23 μm, and 420 nm, respectively. The wavelength of the generated blue beam is also measured with a narrow range grating spectrometer, which is shown in Fig. 2(b). The detected frequency peak is centered at 420.1 nm with the full-width-at-half-maximum of 0.36 nm. This wavelength is precisely corresponding to the $6P_{3/2} \rightarrow 5S_{1/2}$ transition that agrees well with the theoretical expectation.[19] The inset of Fig. 2(b) shows the blue beam profile obtained in a screen and a ruler is used as a reference. The above spatial and spectral measurements confirm that this blue beam is generated by the parametric FWM process. Also, a 5.23 μm field is produced in this process. However, the infrared field is hindered by the opacity of the fused-silica vapor cell window at THz frequencies.

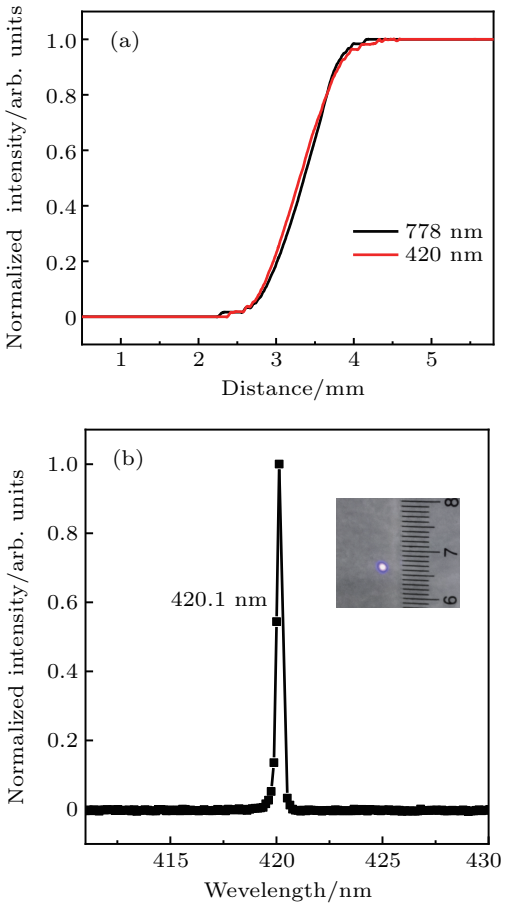

Fig. 2. (a) Knife-edge measurements of the generated CBL beam and the pump beam at the chopper position. (b) Spectrum of the output beam measured by a narrow range grating spectrometer. The inset presents the CBL spatial profile.

The power of the generated blue laser is influenced by several experimental parameters, such as the polarization, power of the pump laser, and the atomic density. The frequency conversion effect is sensitive to the polarization of the pump laser, which determines the transition probability of the excitation pathway. Also, the polarization of the output laser field changes as the polarization of the input laser changes. Here, an efficient CBL generation is achieved when the pump beam has circular polarization instead of linear polarization.[11,13] Thus, we use a pump laser with circular polarization to conduct the experiment in the following research. Angular momentum conservation during the FWM process determines that the polarization of the output CBL is circular with the applied laser fields.[20]

Then, we study the dependence of the generated blue laser power on the atomic density. Figure 3(a) shows the CBL's power as a function of the pump laser frequency and the atomic density, and the white line shows the two-photon transition spectroscopy in vapor A. The pump laser power is fixed at 1.25 W. The temperature of vapor B is varied form 20 °C to 225 °C, which corresponds to an atomic density ranging from 4.04×10^9 cm^{-3} to 2.35×10^{15} cm^{-3}. The measured CBL intensity is plotted with logarithmical atomic density to show the detailed result in the low-density case. As the atomic density increases, the CBL resonances with ^{85}Rb $6P_{3/2} \rightarrow 5S_{1/2}$ ($F = 3$) transition firstly appear. The vapor has two naturally isotopes of ^{85}Rb and ^{87}Rb, whose natural abundances are 73% and 27%, respectively.[21] The statistical weights of the atoms in these hyperfine levels are equal to the degeneracy of the hyperfine levels ($2F + 1$), the ratios of the two hyperfine energy level weight factors of ^{87}Rb and ^{85}Rb are 5 : 3 and 7 : 5, respectively.[22] The large weight factor makes the atoms in $5S_{1/2}$ ($F = 3$) state firstly satisfy the parametric FWM condition. When the atomic density is about 0.2×10^{15} cm^{-3}, the CBL resonances with other three hyperfine transitions appear, and their intensities all increase with the atomic density increasing. When the atomic density is about 0.4×10^{15} cm^{-3}, the CBL intensity begins to decrease due to the self-absorption effect. While the CBL far detuned from the resonance positions can continuously increase as the atomic density increases. The strongest laser generation is observed at red detuning 600 MHz from the ^{85}Rb $5D_{5/2} \rightarrow 5S_{1/2}$ ($F = 2$) transition.

In order to quantitatively study the relationship between CBL's power and atomic density, we measure the laser power with different atomic densities, which is shown in Fig. 3(b). The pump laser frequency is red detuned 600 MHz from the ^{85}Rb $5D_{5/2} \rightarrow 5S_{1/2}$ ($F = 2$) transition. The generated CBL is visually observed when the atomic density reaches 0.5×10^{15} cm^{-3}, and then the CBL's power approximate linearly grows with the increasing atomic density. When the atomic density exceeds 1.75×10^{15} cm^{-3}, the CBL's power growth trend slows down, and tends to saturate. The forward (5S–5P–5D–6P–5S) and reverse (5S–6P–5D–5P–5S) FWM processes are competing with each other. With a larger atom density, the increase of the CBL power causes a balance be-

tween these two FWM processes, which leads to the saturation of the CBL generation.[23] At this point, the parametric FWM process reaches saturation. This saturation point is given by

$$\frac{\Omega_{5S,5P}\,\Omega_{5P,5D}}{\Delta_{5P}} = \frac{\Omega_{5S,6P}\,\Omega_{6P,5D}}{\Delta_{6P}}, \tag{1}$$

where Ω is the Rabi frequency between two states, and Δ_m is the detuning from the state m. For the two-photon excitation scheme used here, the pump laser frequency is largely detuned from the 5P state, thus a microwatts (μW) level blue laser can induce the saturation.

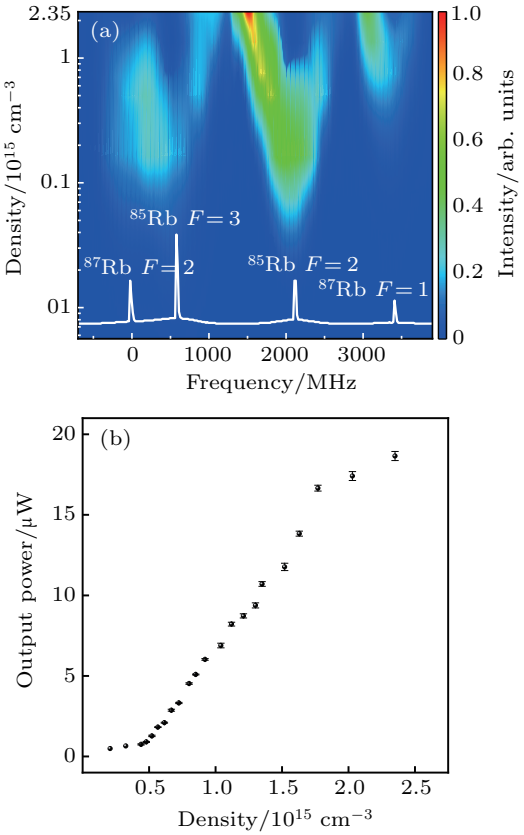

Fig. 3. (a) Contour plots of the generated blue laser intensity as a function of the pump laser frequency detuning and atomic density. The white line shows the two-photon transition spectroscopy in vapor A. (b) The generated CBL power versus atomic density when the pump laser frequency is red detuned 600 MHz from ^{85}Rb $5D_{5/2} \rightarrow 5S_{1/2}$ ($F = 2$) transition.

We also study the effect of the pump laser power on the CBL's power. Figure 4(a) illustrates the CBL's power as a function of the pump laser frequency and power. Here, the atomic density is fixed at a large value of 2.35×10^{15} cm^{-3}. It is found that the CBL's power is weak with a low pump laser power. When the pump power reaches 750 mW, the CBL is observed near the resonance positions. The CBL's power is constantly increasing with the increase of the pump laser power, which seems like the atomic density case in Fig. 3(a). But the CBL frequency position does not change with the increase of the pump laser power, which is different with the atomic density case. With such a high atomic density, the Doppler width is larger than 1 GHz, which gives a large frequency window for the generation of two-photon excitation. While, the generated CBL resonances on 6P → 5S transition have a drastic absorption with such high atomic density. When the pump laser frequency is red detuned about 600 MHz from the ^{85}Rb $5D_{5/2} \rightarrow 5S_{1/2}$ ($F = 2$) transition, the CBL's power reaches the maximum, which can be clearly found in Fig. 4(a). In order to quantitatively study the relationship between CBL's power and pump laser power, we select this detuning position to investigate in detail, which is shown in Fig. 4(b). When the pump laser power reaches the threshold value (about 600 mW) of the FWM process, the blue laser power begins to increase. When the pump laser power keeps increasing, the power of the generated CBL shows a continuous and rapid change. The power of the generated blue laser can be written as[24]

$$P_{\mathrm{CBL}} \propto \frac{\omega_{\mathrm{CBL}}}{\omega_{\mathrm{R}}}\left[\frac{|D_{5S,5P}|\,|D_{5P,5D}|\,\Delta_{6P}}{|D_{5S,6P}|\,|D_{6P,5D}|\,\Delta_{5P}}\right]^2 P_{\mathrm{pump}}^2, \tag{2}$$

where P_{CBL} is the CBL's power, ω_{CBL} and ω_{R} are the frequencies of the 420 nm and 5.23 μm beams, respectively. $|D|$ denotes the dipole matrix element, Δ_m is the detuning from the state m, and P_{pump} is the power of the pump laser. If we continue to increase the pump laser power, the blue laser power

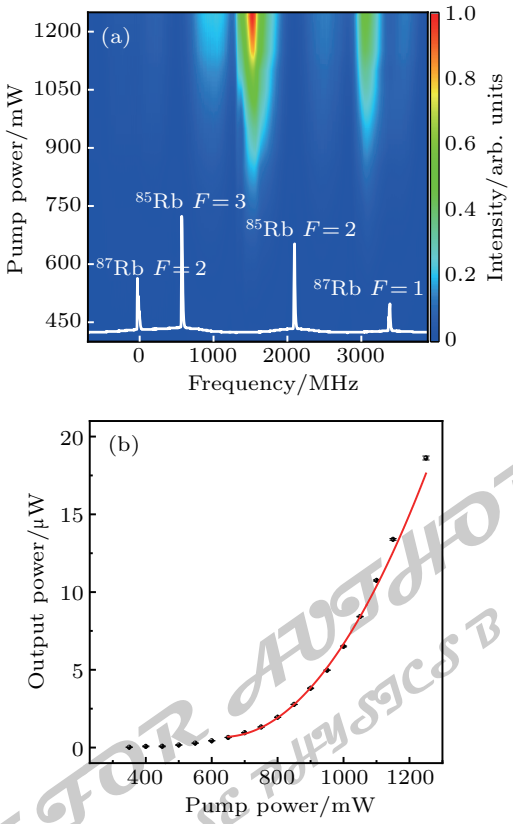

Fig. 4. (a) Contour plots of the generated blue laser power as a function of the pump laser frequency detuning and power. The white line shows the two-photon transition spectroscopy in vapor A. (b) The generated CBL power versus pump laser power when the pump laser frequency is red detuned 600 MHz from ^{85}Rb $5D_{5/2} \rightarrow 5S_{1/2}$ ($F = 2$) transition. The red line is the fitting of the experimental result with formula (2).

is expected to scale as the square of the pump power in the power-broadened regime. The red line is the fitting of the experimental result with formula (2). We obtain a 19 μW blue laser output power with the input pump laser power of 1.25 W. After considering the transmission coefficients of the vapor cell material to the incident laser and blue laser, the blue laser generation efficiency is estimated as 0.0018%. This efficiency is on the order of magnitude from previous experiment with similar mechanism.[16]

Finally, we evaluate the CBL output with optimal experimental parameters. The directly measured profile of the generated CBL is a Gaussian beam, which is shown in the inset of Fig. 5. The beam quality of the CBL can be obtained by measuring the beam waist at different positions. The black squares are results for the x axis, and the red dots are results for the y axis. The measured M^2 values are $M_x^2 = 1.32$ and $M_y^2 = 1.37$, which are similar to those of the 778 nm pump laser. Compared to the frequency up-conversion in the crystals,[25] the blue laser generated in atomic medium has a better beam profile, and the beam quality is good enough for future applications.

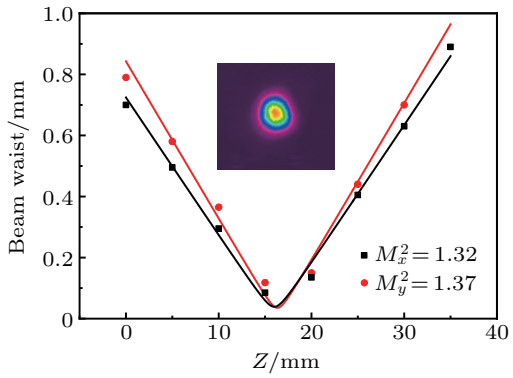

Fig. 5. The measured beam quality M^2 of the output CBL. The black squares and the red dots are the experimental data for the x axis and y axis, respectively. The insert is the beam profile of the CBL.

4. Conclusion

In summary, we have studied the parametric FWM process in a Rb vapor by using a single 778 nm laser. The coherence of the generated 420 nm light is firstly confirmed by the spatial and spectral measurements of the laser by the knife-edge method and a narrow range grating spectrometer. A circularly polarized pump beam, which leads to a higher transition probability determined by selection rules, promises an efficient CBL generation. The CBL's power is found to be approximate linearly increase with the increase of the atomic density and a saturation effect is observed when the atomic density exceeds 1.75×10^{15} cm^{-3}. The CBL's power has a quadratic dependence on the pump laser power after the pump laser's power exceeds the threshold value of the FWM process. These results are qualitatively interpreted and discussed in theory. Finally, a 19 μW blue laser output with the beam quality of $M_x^2 = 1.32$, $M_y^2 = 1.37$ is obtained. Due to its good optical characteristics, this laser can be used in the realization of single photon source and measurement of material properties. Such results enrich our understanding of the dynamic mechanism of parametric FWM process in atomic medium and have great prospect in the applications of novel tunable laser source and underwater optical communication. In the next work, we will use an improved multiple-pass metal vapor cell to improve the blue laser generation efficiency. In addition, if we further use a buildup cavity surrounding the atomic medium, the output power can be greatly increased, and the beam quality can also be optimized.[26]

References

[1] Lü B L, Burkett W H and Xiao M 1998 *Opt. Lett.* **23** 0146
[2] Fleischhauer M, Imamoglu A and Marangos J P 2005 *Rev. Mod. Phys.* **77** 0034
[3] Scully M O and Zhu S Y 1989 *Phys. Rev. Lett.* **62** 2814
[4] Ding D S, Zhou Z Y and Shi B S 2013 *Chin. Phys. B* **22** 114203
[5] Radnaev A G, Dudin Y O, Zhao R, Jen H H, Jenkins S D, Kuzmich A and Kennedy T A B 2010 *Nat. Phys.* **6** 894
[6] Michelle S M, Daniel J G and Robert W B 1985 *Phys. Rev. Lett.* **55** 1086
[7] Brustlein S, Rio D L, Tonello A, Delage L and Reynaud F 2008 *Phys. Rev. Lett.* **100** 153903
[8] Abbas M M, Mumma M J, Kostiuk T and Buhl D 1976 *Appl. Optics* **15** 427
[9] Smith R C and Baker K S 1981 *Appl. Optics* **20** 177
[10] Wang L R, Zhang Y C, Xiang S S, Cao S K, Xiao L T and Jia S T 2015 *Chin. Phys. B* **24** 063201
[11] Kargapol'tsev S V, Velichansky V L, Yarovitsky A V, Taichenachev A V and Yudin V I 2005 *Quantum Electron.* **31** 591
[12] Zibrov A S, Lukin M D, Hollberg L and Scully M O 2001 *Phys. Rev. A* **65** 051801(R)
[13] Schultz J T, Abend S, Döring D, Debs J E, Altin P A, White J D, Robins N P and Close1 J D 2009 *Opt. Lett.* **34** 2321
[14] Akulshin A M, Orel A A and McLean R J 2012 *J. Phys. B: At. Mol. Opt. Phys.* **45** 015401
[15] Sulham C V, Pitz G A and Perram G P 2010 *Appl. Phys B* **101** 57
[16] Brekke E and Alderson L 2013 *Opt. Lett.* **38** 2147
[17] Skinner D R and Whitcher R E 1972 *J. Phys. E: Sci. Instrum.* **5** 237
[18] Khosrofian J M and Garetz B A 1983 *Appl. Optics* **22** 3406
[19] Šibalić N, Pritchard J D, Adams C S and Weatherill K J 2017 *Comput. Phys. Commun.* **220** 319
[20] Cheng X M, Du Y G, Zhang Y P, Wang Z G, Miao Y Z, Ren Z Y and Bai J T 2012 *Opt. Commun.* **285** 4507
[21] Cheng J T, Edwards J C and Ellis P L 1990 *J. Phys. Chem.* **94** 553
[22] Nieddu T, Ray T, Rajasree K S, Roy R and Chormaic S N 2019 *Opt. Express* **27** 6528
[23] Garrett W R, Hart R C, Moore M A and Payne M G 1990 *Phys. Rev. A* **41** 6345
[24] Brekke E and Swan N 2019 *J Opt. Soc. Am. B* **36** 421
[25] Akbari R and Major A 2013 *Laser Phys* **23** 035401
[26] Brekke E and Potier S 2017 *Appl. Optics* **56** 1559

Chinese Physics B

Volume 29 Number 4 April 2020

(*Continued on the Bookbinding Inside Back Cover*)

ATOMIC AND MOLECULAR PHYSICS

CONDENSED MATTER: ELECTRONIC STRUCTURE, ELECTRICAL, MAGNETIC, AND OPTICAL PROPERTIES